Non-equilibrium Phenomena in attractive BEC's:
Solitons, Fragmentons, CATons,...

Alexej I. Streltsov

Theoretische Chemie, Physikalisch-Chemisches Institut, Universität Heidelberg

Im Neuenheimer Feld 229, D-69120 Heidelberg, Germany

Frontiers of Ultracold Atoms and Molecules

Kavli Institute for Theoretical Physics

University of California, Santa Barbara, USA, October 14, 2010

Problem: N *interacting* bosons in a trap

PRL 99, 030402 (2007), PRA 77, 033613 (2008)

- Hamiltonian

$$\hat{\mathrm{H}} = \sum_{i=1}^{N} \hat{h}(x_i, t) + \sum_{i \neq j} W(x_i, x_j)$$

  - $\hat{h}(x_i) = \hat{T} + \hat{V}(x_i, t)$
  - $V(x_i)$ external trap potential
  - $W(x_i,x_j)$ two-particle interaction potential
    - $\lambda_0\ \delta(x_i - x_j)$ – contact interaction $\lambda_0 \sim \mathbf{a_s}$ $\mathbf{a_s}$- *s*-wave scattering length

- Time-dependent many-body Schrödinger Equation

$$i\hbar \frac{\partial}{\partial t} \Psi(\mathbf{x}, t) = \hat{\mathrm{H}}\, \Psi(\mathbf{x}, t)$$

- One has to specify initial condition

$$\Psi(\mathbf{x}, t=0) = \Psi(x_1, x_2, \ldots, x_{\mathrm{N}}, t=0)$$

- and propagate $\Psi(x,t) \longrightarrow \Psi(x,t+\Delta t)$

MCTDHB: Key idea

N identical bosons **PRL 99, 030402 (2007), PRA 77, 033613 (2008)**

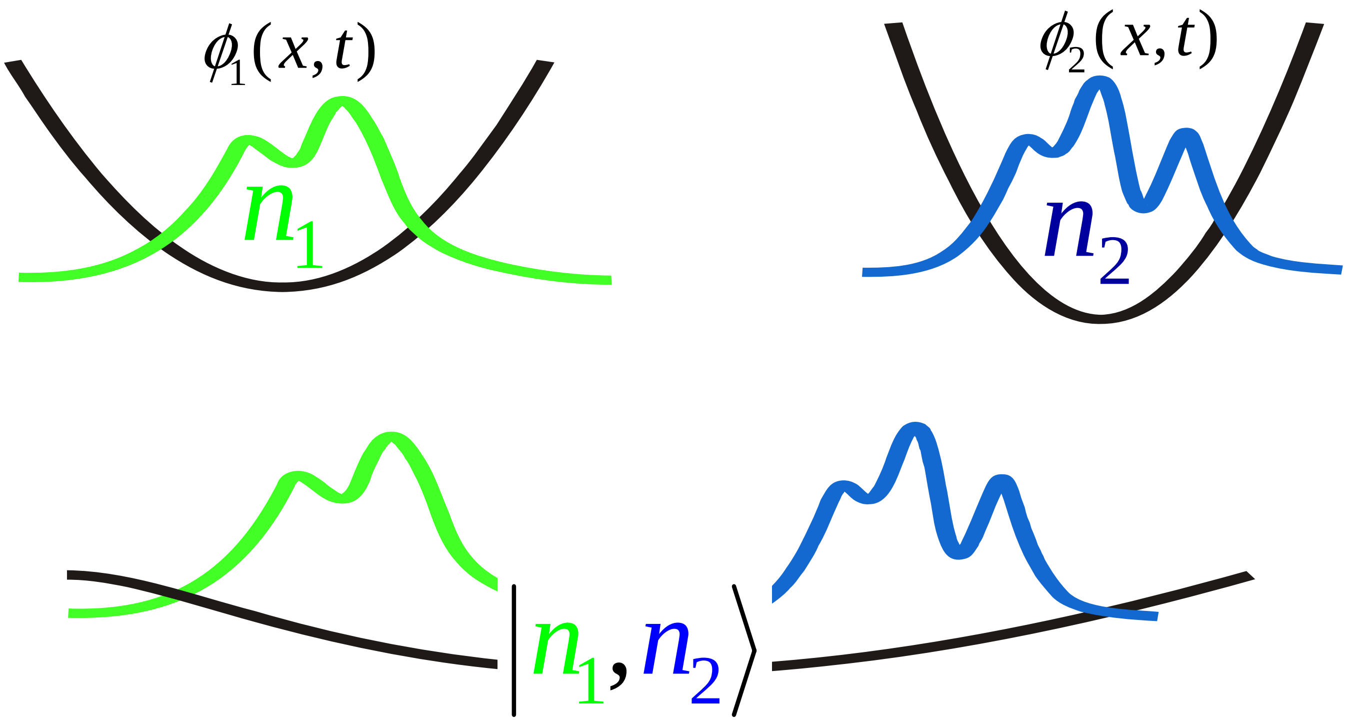

$$\cdots C_{n_1-1,n_2+1}(t)\,|n_1-1, n_2+1\rangle + C_{n_1,n_2}(t)\,|n_1, n_2\rangle + C_{n_1+1,n_2-1}(t)\,|n_1+1, n_2-1\rangle \cdots$$

Orbitals ϕ's and expansion coefficients C_{n_1,n_2}'s are time dependent, i.e., change during the evolution

MCTDHB: Ideology

N identical bosons **PRL 99, 030402 (2007), PRA 77, 033613 (2008)**

MCTDHB(M) ansatz for wave-function:
linear combination of time-dependent permanents

$$\Psi_{MCTDHB(M)} = \sum_{i_1,i_2,\cdots,i_M}^{F_N^M} C_{i_1,i_2,\cdots,i_M}(t)\, \Phi_{i_1 i_2 \ldots i_M}(x_1,\ldots,x_N,t) = \sum_{i_1,i_2,\cdots,i_M}^{F_N^M} C_{i_1,i_2,\cdots,i_M}(t)\,|\, i_1 i_2 i_3 i_4 \cdots i_M ; t\rangle$$

Every permanent $|\, \boldsymbol{i_1\, i_2\, i_3\, i_4 \cdots i_M ; t} \rangle$

is symmetryzed time-dependent Hartree product

$$\Phi_{i_1 i_2 i_3 i_4 \ldots i_M}(x_1,x_2,\ldots,x_N,t) = \hat{S}\, \underbrace{\phi_1(x_1,t)\cdots\phi_1(x_{i_1},t)}_{i_1}\cdots\underbrace{\phi_2(x_{i_1+i_2},t)}_{i_2}\cdots\underbrace{\phi_M(x_{N-i_M},t)\cdots\phi_M(x_N,t)}_{i_M}$$

Limiting one-configurational **MCTDHB(M=1)** case gives
the famous Gross-Pitaevskii mean-field

$$\Psi_{GP\equiv\ MCTDHB(1)} = \phi(x_1,t)\phi(x_2,t)\phi(x_3,t)\ldots\phi(x_N,t) \rightarrow \left| N;t \right\rangle$$

MCTDHB: Methodology

$\Psi(t) \rightarrow \Psi(t+\Delta t)$ PRL 99, 030402 (2007), PRA 77, 033613 (2008), PRA 81, 022124 (2010)

$$\Psi_{MCTDHB(M)} = \sum_{i_1,i_2,i_3,\cdots,i_M}^{F_N^M} C_{i_1,i_2,i_3,\cdots,i_M}(t)\,|\,i_1 i_2 i_3 \cdots i_M ; t\rangle$$

$$\Psi_{GP\equiv MCTDHB(1)} = C_N\,|\,N;t\rangle,\; C_N \equiv 1$$

$$\begin{bmatrix} C_{i_1,i_2,i_3,\cdots,i_M}(t) \\ \left| \begin{matrix} \phi_1(x,t) \\ \phi_2(x,t) \\ \cdots \\ \phi_M(x,t) \end{matrix} \right\rangle \end{bmatrix} \rightarrow \begin{bmatrix} C_{i_1,i_2,i_3,\cdots,i_M}(t+\Delta t) \\ \left| \begin{matrix} \phi_1(x,t+\Delta t) \\ \phi_2(x,t+\Delta t) \\ \cdots \\ \phi_M(x,t+\Delta t) \end{matrix} \right\rangle \end{bmatrix}$$

$$\phi_{GP}(x,t) \rightarrow \phi_{GP}(x,t+\Delta t)$$

$$\left\{ \begin{array}{l} \boxed{MCTDHB\;\; for\;\; C_{i_1,i_2,\cdots,i_3,i_M}(t)} = \dfrac{\partial \vec{C}(t)}{\partial t} \\[2ex] \boxed{MCTDHB\;\; for \left| \begin{matrix} \phi_1(x,t) \\ \phi_2(x,t) \\ \cdots \\ \phi_M(x,t) \end{matrix} \right\rangle} = \left| \begin{matrix} \partial\phi_1(x,t)/\partial t \\ \partial\phi_2(x,t)/\partial t \\ \cdots \\ \partial\phi_M(x,t)/\partial t \end{matrix} \right\rangle \end{array} \right.$$

$$\boxed{GP\;\; for\;\; \phi_{GP}(x,t)} = \frac{\partial \phi_{GP}(x,t)}{\partial t}$$

REVIEW

Optical Spatial Solitons and Their Interactions: Universality and Diversity

George I. Stegeman[1] and Mordechai Segev[2,3]

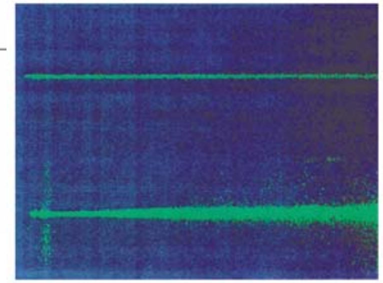

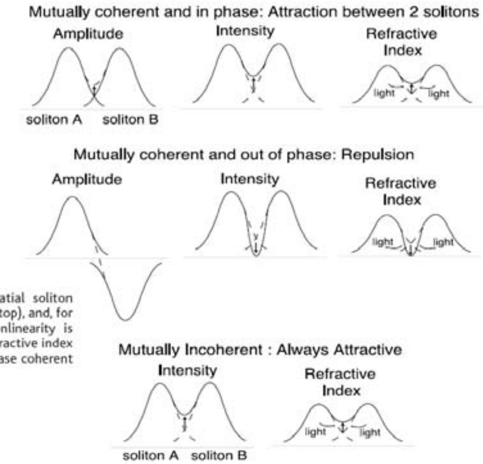

Fig. 2 (above). A top view photograph of a 10-μm-wide spatial soliton propagating in a strontium barium niobate photorefractive crystal (top), and, for comparison, the same beam diffracting naturally when the nonlinearity is "turned off" (bottom). (*23*). **Fig. 3 (right).** Schematic of the refractive index spatial distribution for a collision between in-phase and out-of-phase coherent spatial solitons.

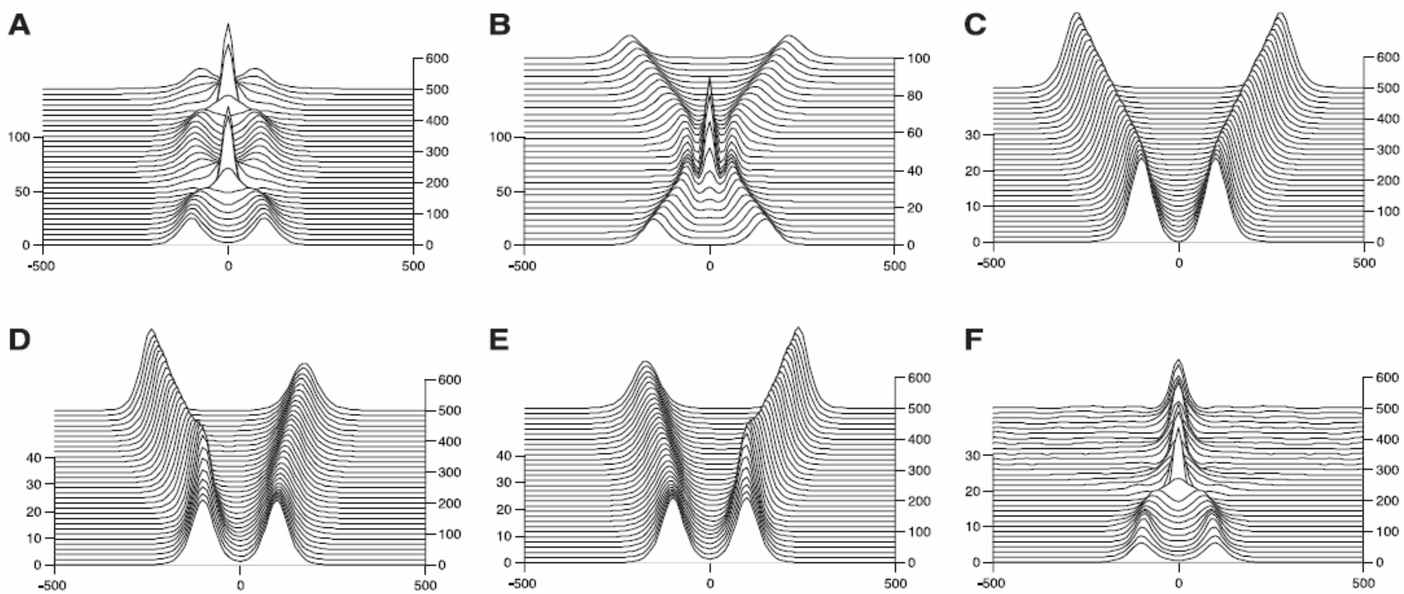

Fig. 4. Beam evolution calculations of the interactions between two solitons for the following cases: (**A**) Parallel input trajectories, in-phase Kerr solitons; (**B**) converging input trajectories, in-phase Kerr solitons; (**C**) parallel input trajectories, out-of-phase Kerr solitons; (**D**) parallel input trajectories, $\pi/2$ relative phase between Kerr solitons; (**E**) parallel input trajectories, $3\pi/2$ relative phase between Kerr solitons; and (**F**) fusion of two solitons input on parallel trajectories in saturating nonlinear media for "small" input separations.

Formation and propagation of matter-wave soliton trains

Kevin E. Strecker*, **Guthrie B. Partridge***, **Andrew G. Truscott***† **& Randall G. Hulet***

* *Department of Physics and Astronomy and Rice Quantum Institute, Rice University, Houston, Texas 77251, USA*

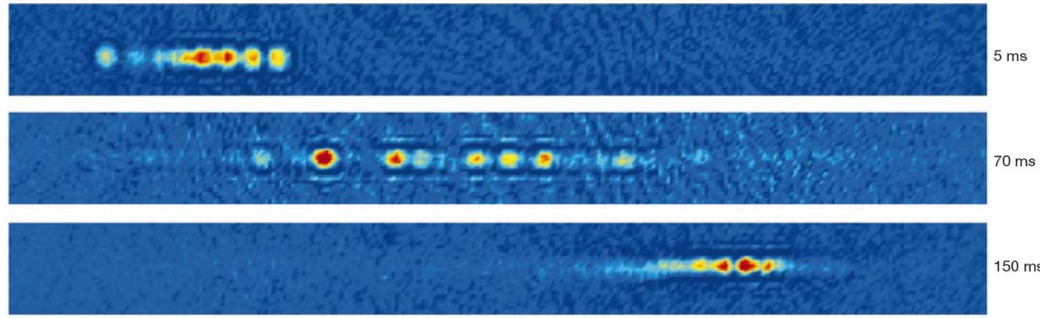

Figure 4 Repulsive interactions between solitons. The three images show a soliton train near the two turning points and near the centre of oscillation. The spacing between solitons is compressed at the turning points, and spread out at the centre of the oscillation. A simple model based on strong, short-range, repulsive forces between nearest-neighbour solitons indicates that the separation between solitons oscillates at approximately twice the trap frequency, in agreement with observations. The number of solitons varies from image to image because of shot to shot experimental variations, and because of a very slow loss of soliton signal with time. As the axial length of a soliton is expected to vary as $1/N$ (ref. 11), solitons with small numbers of atoms produce particularly weak absorption signals, scaling as N^2. Trains with missing solitons are frequently observed, but it is not clear whether this is because of a slow loss of atoms, or because of sudden loss of an individual soliton.

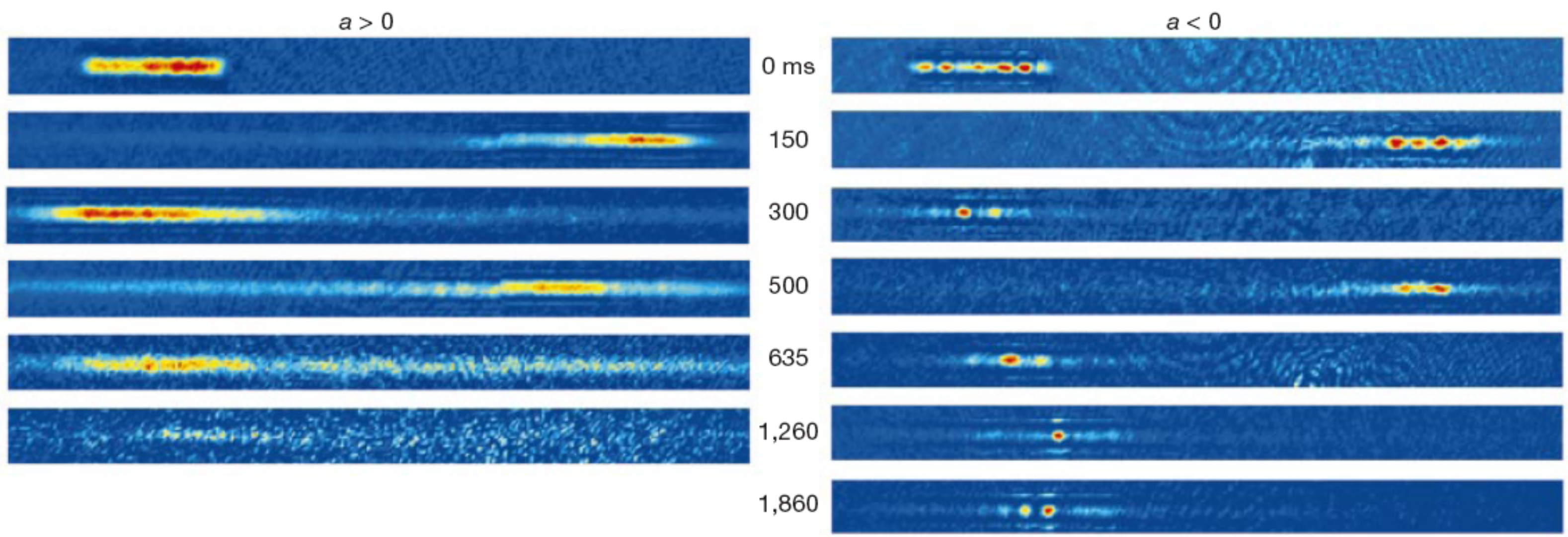

Figure 3 Comparison of the propagation of repulsive condensates with atomic solitons. The images are obtained using destructive absorption imaging, with a probe laser detuned 27 MHz from resonance. The magnetic field is reduced to the desired value before switching off the end caps (see text). The times given are the intervals between turning off the end caps and probing (the end caps are on for the $t = 0$ images). The axial dimension of each image frame corresponds to 1.28 mm at the plane of the atoms. The amplitude of oscillation is $\sim$370 μm and the period is 310 ms. The $a > 0$ data correspond to 630 G, for which $a \approx 10a_0$, and the initial condensate number is $\sim 3 \times 10^5$. The $a < 0$ data correspond to 547 G, for which $a \approx -3a_0$. The largest soliton signals correspond to $\sim$5,000 atoms per soliton, although significant image distortion limits the precision of number measurement. The spatial resolution of $\sim$10 μm is significantly greater than the expected transverse dimension $l_r \approx 1.5$ μm.

Formation of a Matter-Wave Bright Soliton

L. Khaykovich,[1] F. Schreck,[1] G. Ferrari,[1,2] T. Bourdel,[1]
J. Cubizolles,[1] L. D. Carr,[1] Y. Castin,[1] C. Salomon[1*]

We report the production of matter-wave solitons in an ultracold lithium-7 gas. The effective interaction between atoms in a Bose-Einstein condensate is tuned with a Feshbach resonance from repulsive to attractive before release in a one-dimensional optical waveguide. Propagation of the soliton without dispersion over a macroscopic distance of 1.1 millimeter is observed. A simple theoretical model explains the stability region of the soliton. These matter-wave solitons open possibilities for future applications in coherent atom optics, atom interferometry, and atom transport.

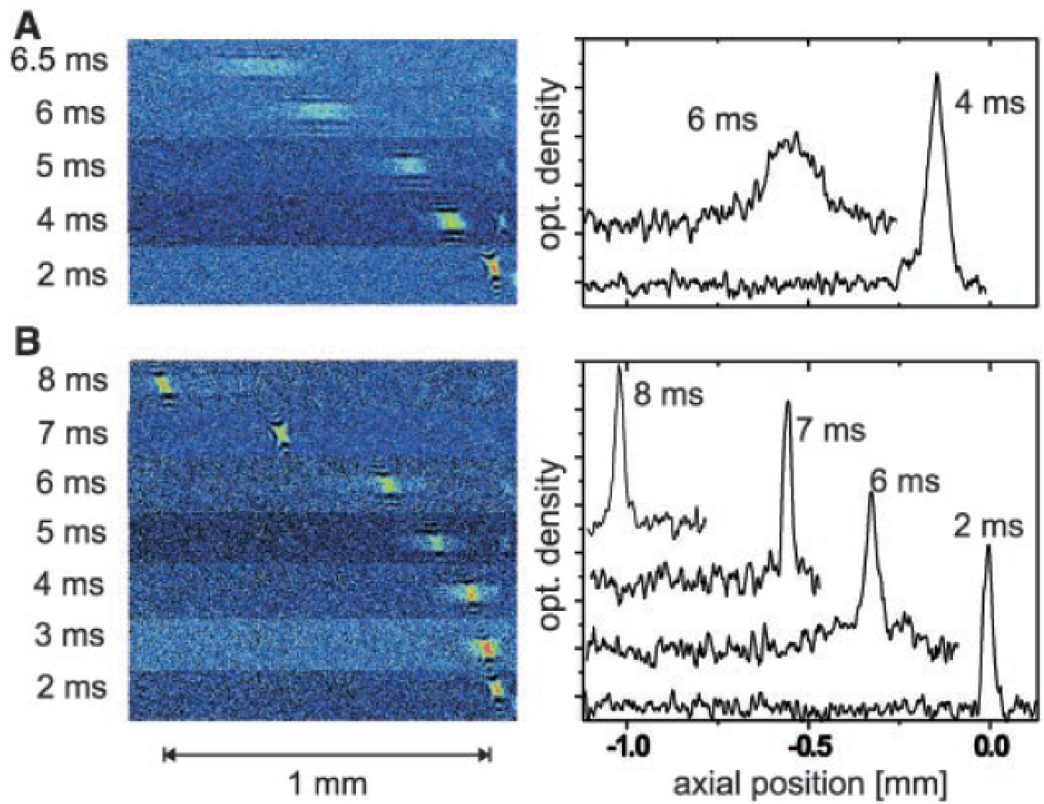

Fig. 3. Absorption images at variable delays after switching off the vertical trapping beam. Propagation of an ideal BEC gas (**A**) and of a soliton (**B**) in the horizontal 1D waveguide in the presence of an expulsive potential. Propagation without dispersion over 1.1 mm is a clear signature of a soliton. Corresponding axial profiles are integrated over the vertical direction.

Formation of Bright Matter-Wave Solitons during the Collapse of Attractive Bose-Einstein Condensates

Simon L. Cornish,[1,*] Sarah T. Thompson,[2] and Carl E. Wieman[2]

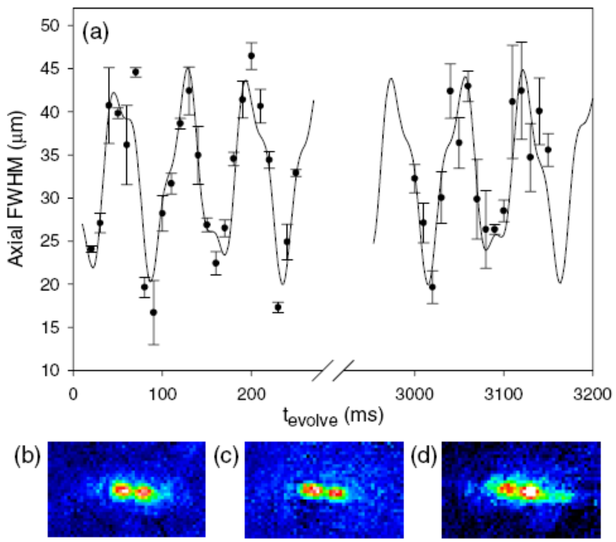

FIG. 2 (color online). Observation of solitons oscillating in the magnetic trap following the collapse at $a_{collapse} = -11.4a_0$ of condensates initially containing approximately 8000 atoms. (a) The evolution of the axial (horizontal) FWHM of the remnant condensate obtained from a single Gaussian fit to the images. Above the resolution limit of the imaging system, the remnant condensate is observed to separate into two solitons as shown in the images taken at (b) 210 ms, (c) 1140 ms, and (d) 3110 ms. Each image is $77 \times 129\ \mu$m. The error bars represent the statistical spread in the data only.

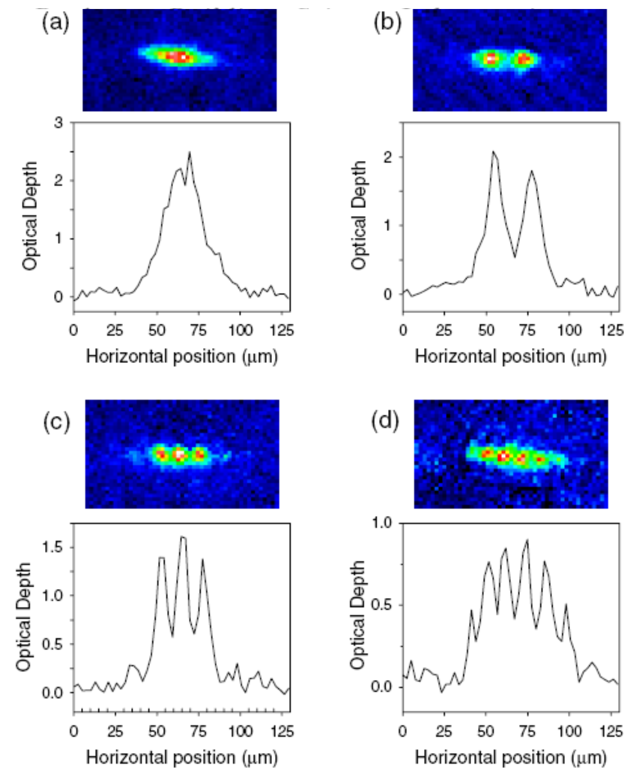

FIG. 3 (color online). Images and cross sections of remnant condensates. (a) When the magnitude of $a_{collapse}$ is sufficiently small a single remnant condensate containing less than the critical number is observed to survive the collapse. When the magnitude of $a_{collapse}$ is larger and/or larger initial condensates are used, the remnant condensate is observed to split into a number of solitons determined by the conditions of the collapse (b)–(d). Each image is $77 \times 129\ \mu$m.

Formation and dynamics of fragmented attractive condensates in 1D

Fragmentons

A.I.S, O.E. Alon, and L.S. Cederbaum,
Phys. Rev. Lett. 100, 130401 (2008)

Time-evolutions of initially-coherent wave packet: GP (upper) versus Many-Body (bottom)

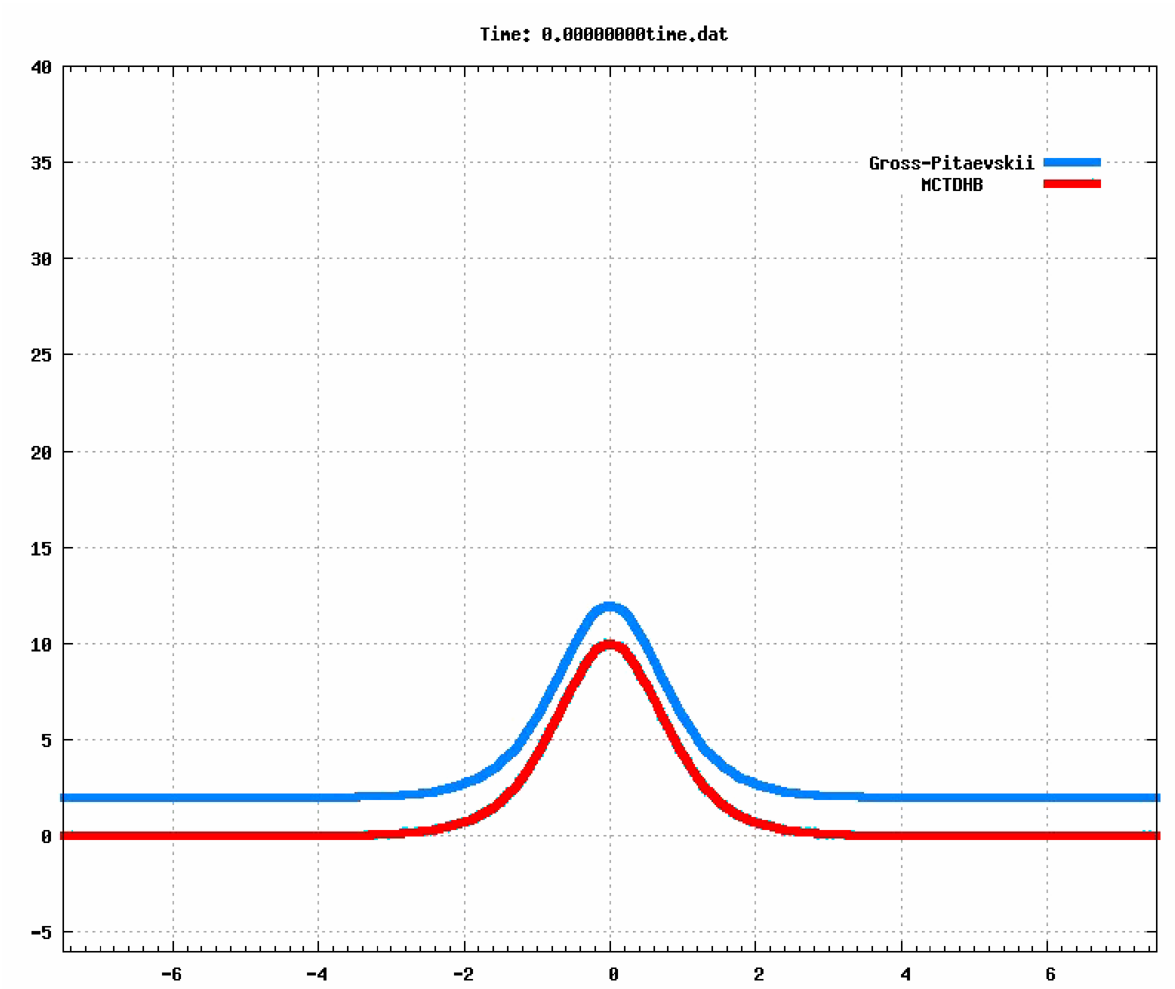

1D system of N=1000 attractive bosons (λ_0=-0.008)

The initial wave packets are **COHERENT** (*sech[γx]*)

Gross-Pitaevskii

- breathing dynamics

Many-body

- breathing dynamics
- attempts to split or splitting

Time-evolutions of initially-coherent wave packets: Many-Body (left) versus GP (right)

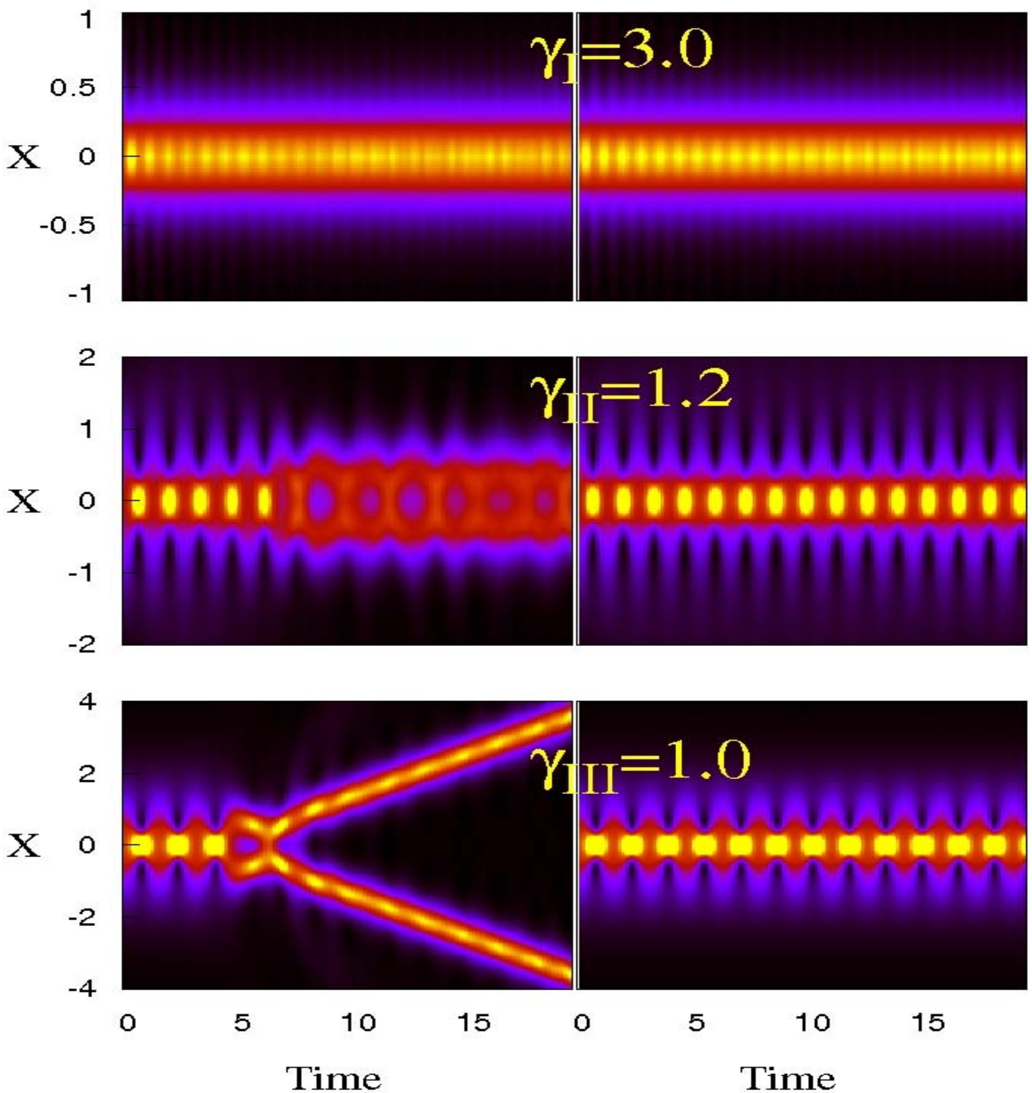

1D system of N=1000 attractive bosons (λ_0=-0.008)

The initial wave packets are **COHERENT** (*sech[γx]*)

Gross-Pitaevskii

- breathing dynamics

Many-body

- breathing dynamics
- attempts to split or splitting

Analysis of the evolving Many-Body wave packets

Reduced one-body density matrix $\rho(x,x',t)$ is diagonalized

$$\rho(x,t) = n_1(t)\left|\phi_1^{NO}(x,t)\right|^2 + n_2(t)\left|\phi_2^{NO}(x,t)\right|^2$$

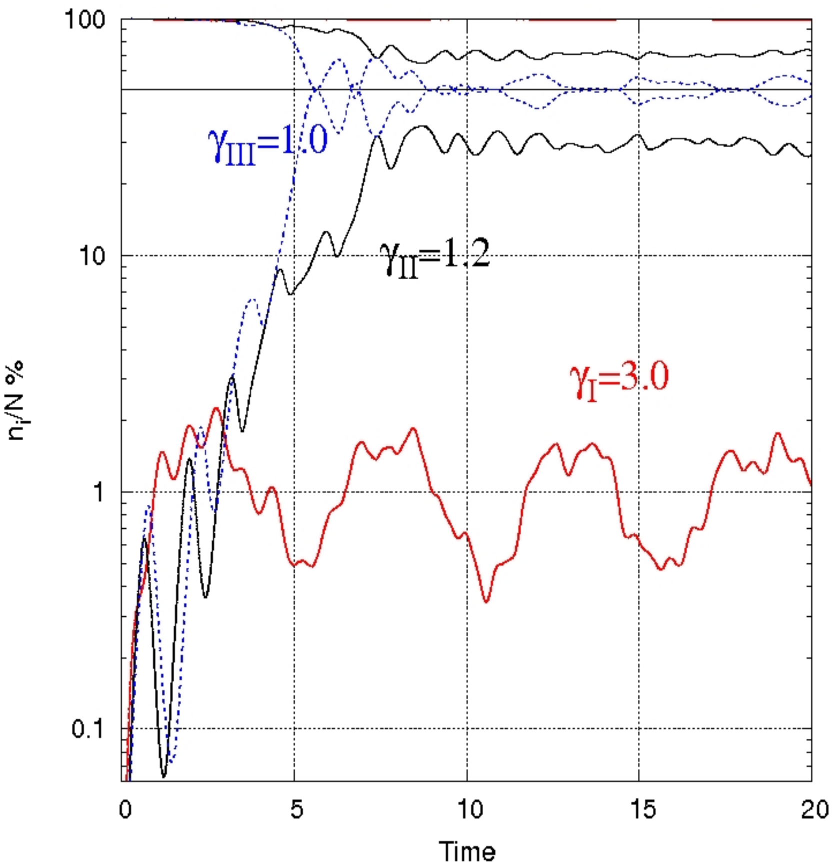

Eigenfunctions (natural orbitals) $\phi_1^{NO}(x,t),\ \phi_2^{NO}(x,t)$

Eigenvalues (natural occupation numbers): $n_1(t),\ n_2(t)$

Time evolution of the natural occupation numbers (log scale in %)

Mean-field energy diagram for interpretation of the Fragmenton

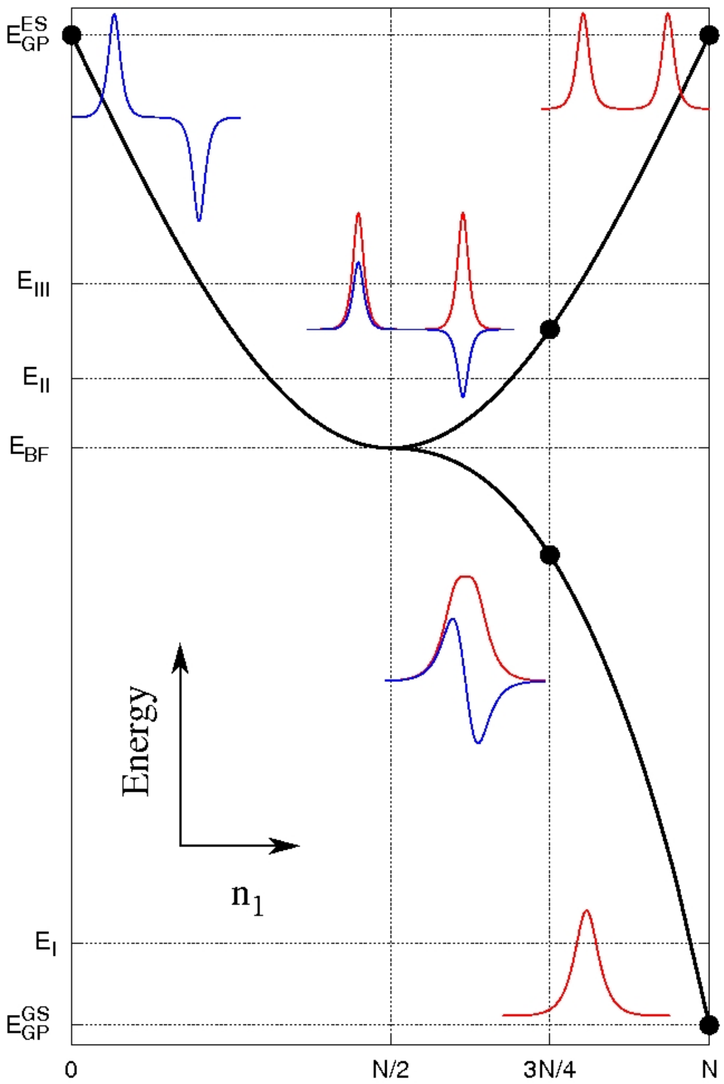

Two-fold fragmented state $|n_1,n_2\rangle$ is built up using delocalised orbitals:

$$\phi_{1,2} \propto \{\mathrm{sech}[\gamma_m(x-X_0)] \pm \mathrm{sech}[\gamma_m(x+X_0)]\}$$

For every given n_1 ($n_2=N-n_1$), mean-field energy $\langle n_1,n_2|H|\,|n_1,n_2\rangle$ is minimized with respect to γ_m and X_0

Two-orbital mean-field energy functional

$$E(n_1) = n_1 h_{11} + \frac{\lambda_0 n_1(n_1-1)}{2}\int|\phi_1|^4 dx + n_2 h_{22} + \frac{\lambda_0 n_2(n_2-1)}{2}\int|\phi_2|^4 dx + 2\lambda_0 n_1 n_2 \int|\phi_1|^2|\phi_2|^2 dx$$

- ✓ Upper branch : two well-separated, but entangled parts
- ✓ Lower branch : all bosons stay localized in one cloud

Conclusions on attractive condensates in 1D and elongated 2D traps

- ✓ *The initially coherent wave-packet can dynamically dissociate into two parts when its energy exceeds a threshold value*
- ✓ *The time-dependent GP theory applied to the same initial state does not show up the splitting*
- ✓ *The split object fragmenton possesses remarkable properties:*

(1) two-fold fragmented, i.e., not coherent

(2) dynamically stable, i.e., it propagates almost without dispersion

(3) delocalized, i.e., two dissociated parts still communicate with one another

Formation of dynamical Schrödinger cats in low-dimensional ultracold attractive Bose gases

CATons I

A.I.S, O.E. Alon, and L.S. Cederbaum,
Phys. Rev. A 80, 043616 (2009) (arXiv:0812.3573)

Scattering of an attractive BEC from a barrier

Initial packet: at x=0, **velocity** $\vec{v} = -0.5$; **Barrier:** at x=-3, V_0=0.4, width σ= *0.15*

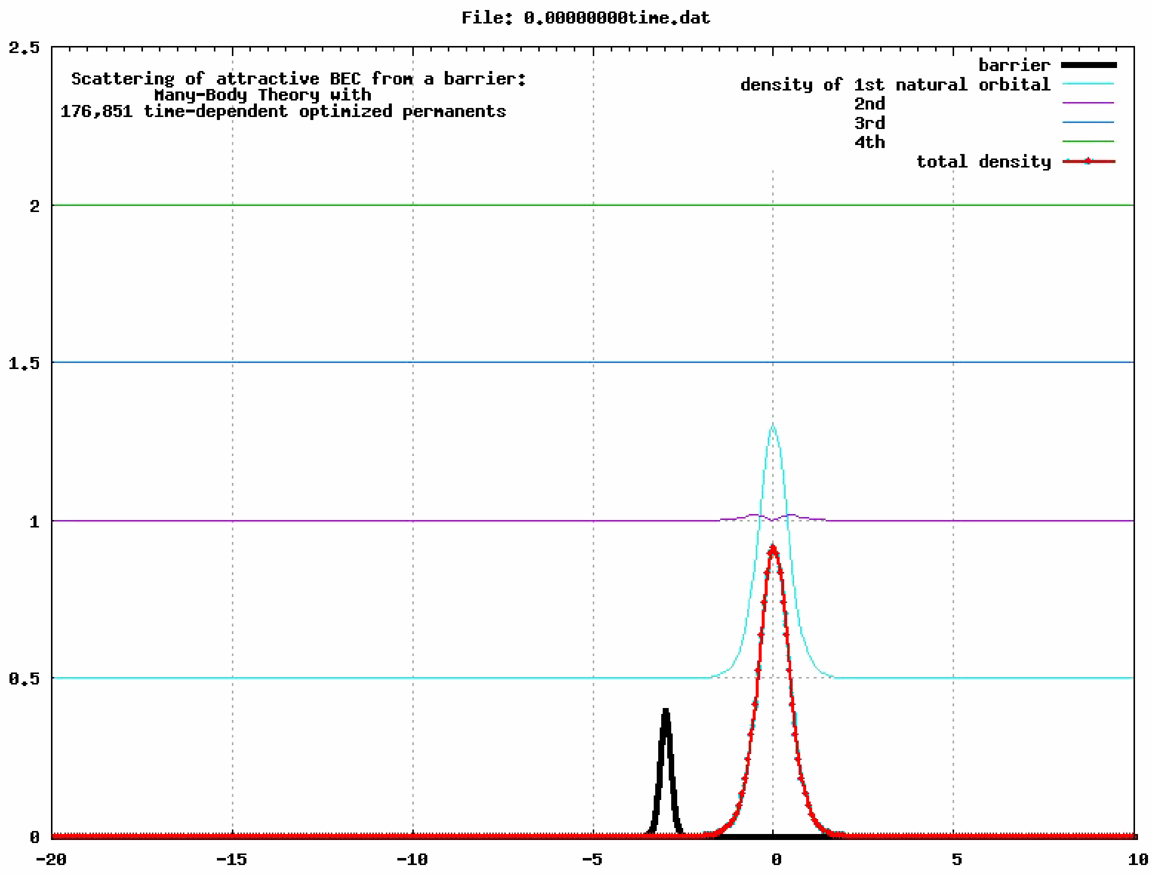

Time-dependent Schrödinger cat state (CATon) is formed

Initial wave-packet location at x=0, velocity $\vec{v} = -0.5$

Barriers: location at x=-3, V_0=0.4, **three different barrier widths**

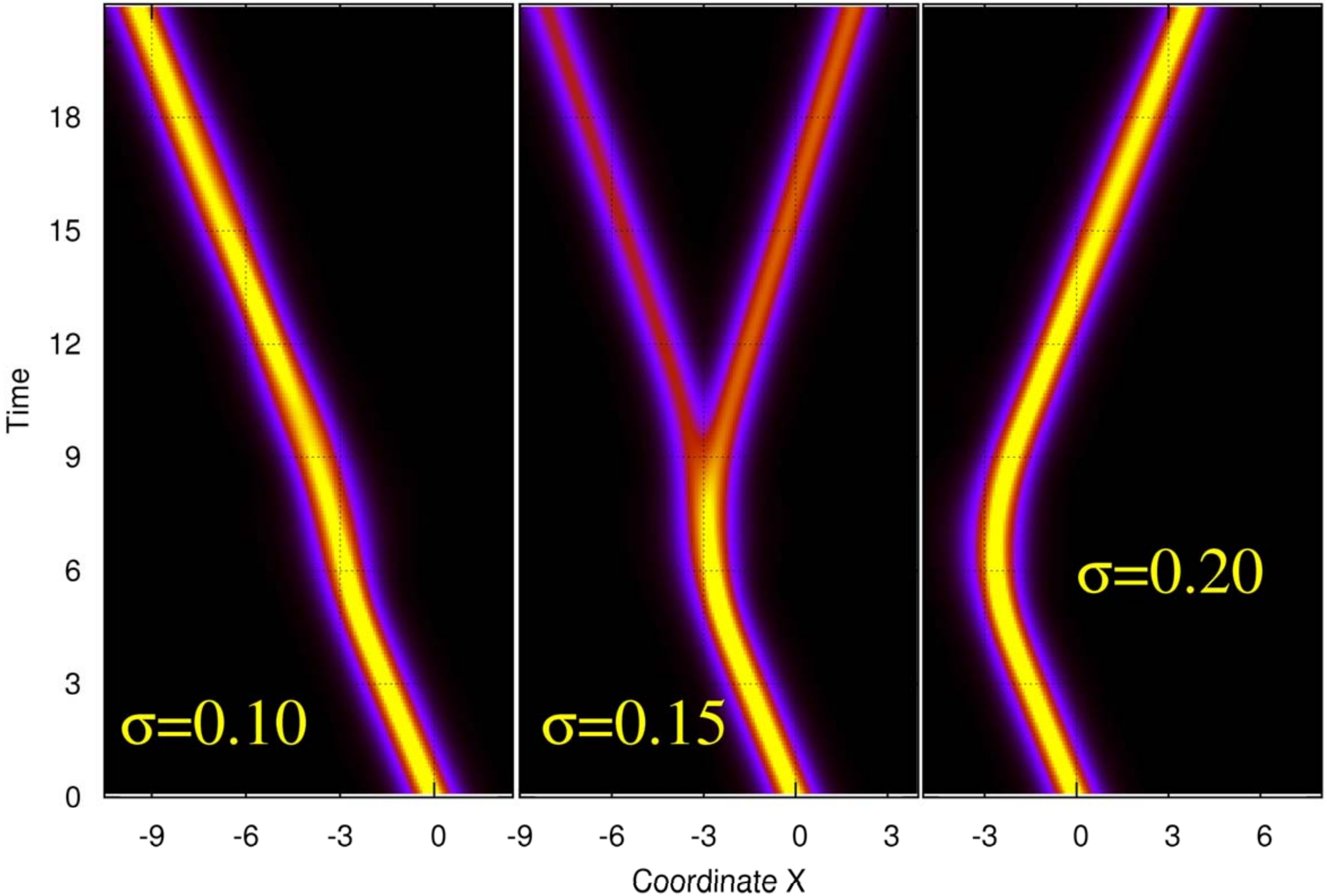

σ= 0.10 – Full transmission case

σ= 0.15 – Split case

σ= 0.20 – Full reflection case

GP propagation of Sech[1.98x] velocity $\vec{v} = -0.5$

Barriers: location at x=-3, V_0=0.4, **three different barrier widths**

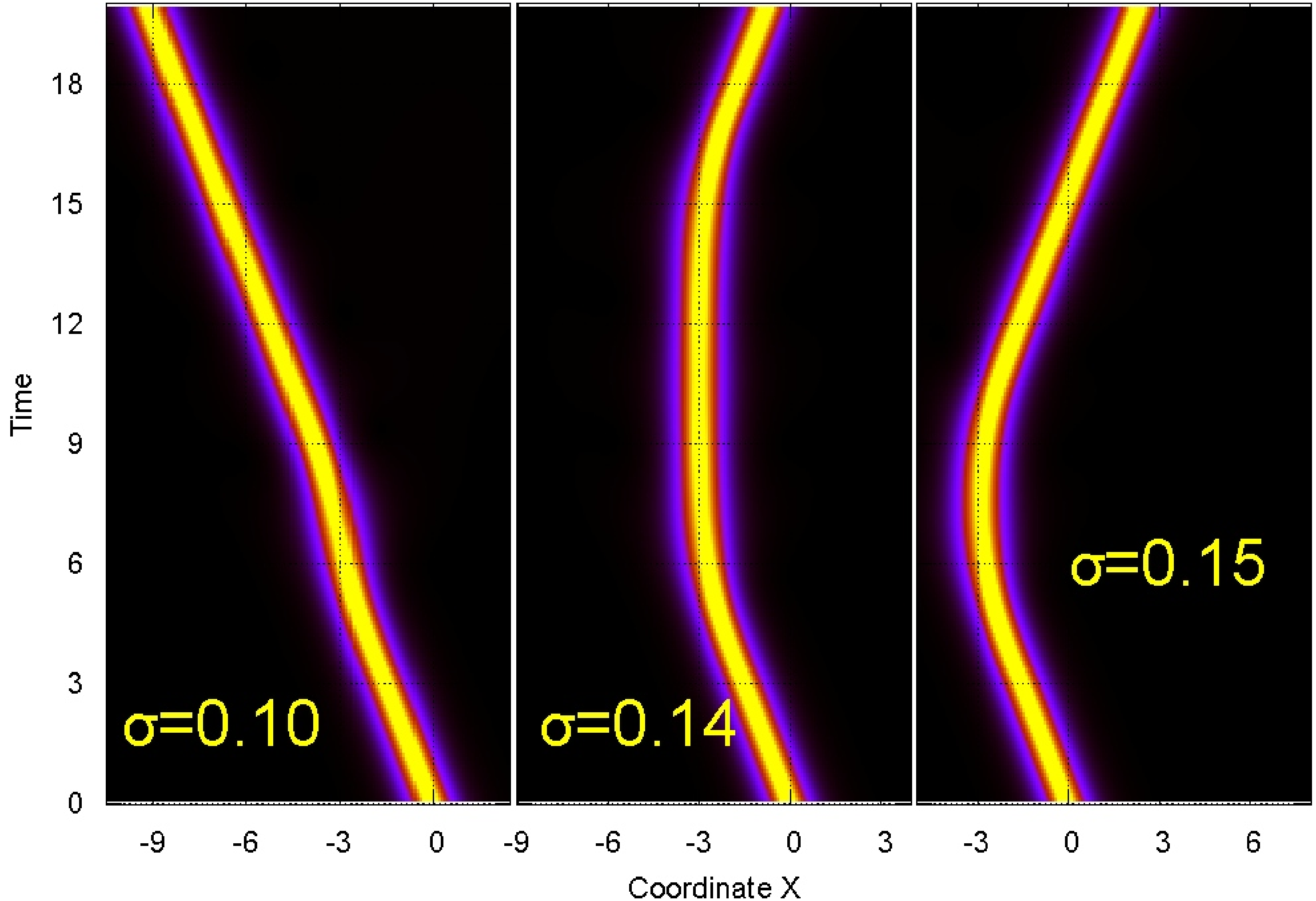

σ= 0.10 – Full transmission case

σ= 0.14 – Long-lived case

σ= 0.15 – Full reflection case

Analysis of the evolving Many-Body wave packets

Reduced one-body density matrix $\rho(x,x',t)$ is diagonalized

$$\rho(x,t)=\rho_1(t)\left|\phi_1^{NO}(x,t)\right|^2+\rho_2(t)\left|\phi_2^{NO}(x,t)\right|^2$$

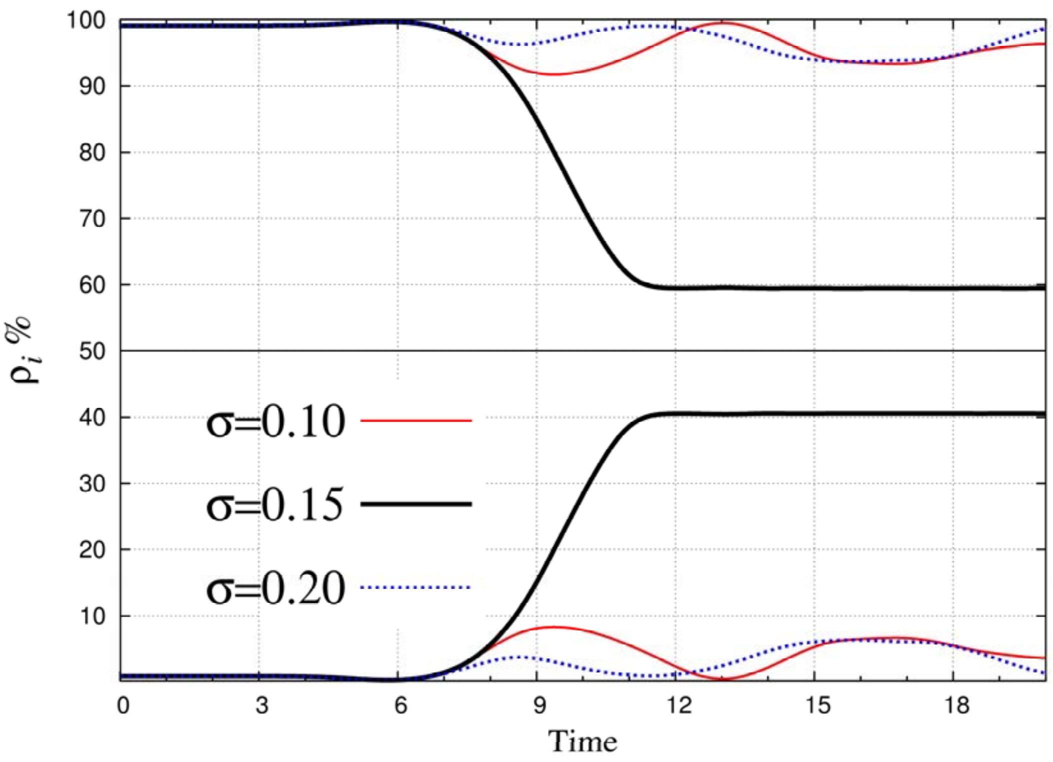

At t=0 all wave-packets are condensed: ρ_1=99.1%

Remain mainly condensed:

σ=0.10 - full transmission,

σ=0.20 - full reflection cases

Becomes fragmented:

σ=0.15 – split case,

at t=15: ρ_1=59.5% and ρ_2=40.5%

Analysis of split case
(proof that the split object is a Schrödinger cat state)

Fock space is spanned by: |N,0›,|N-1,1›,...,|1,N-1›,|0,N› configurations

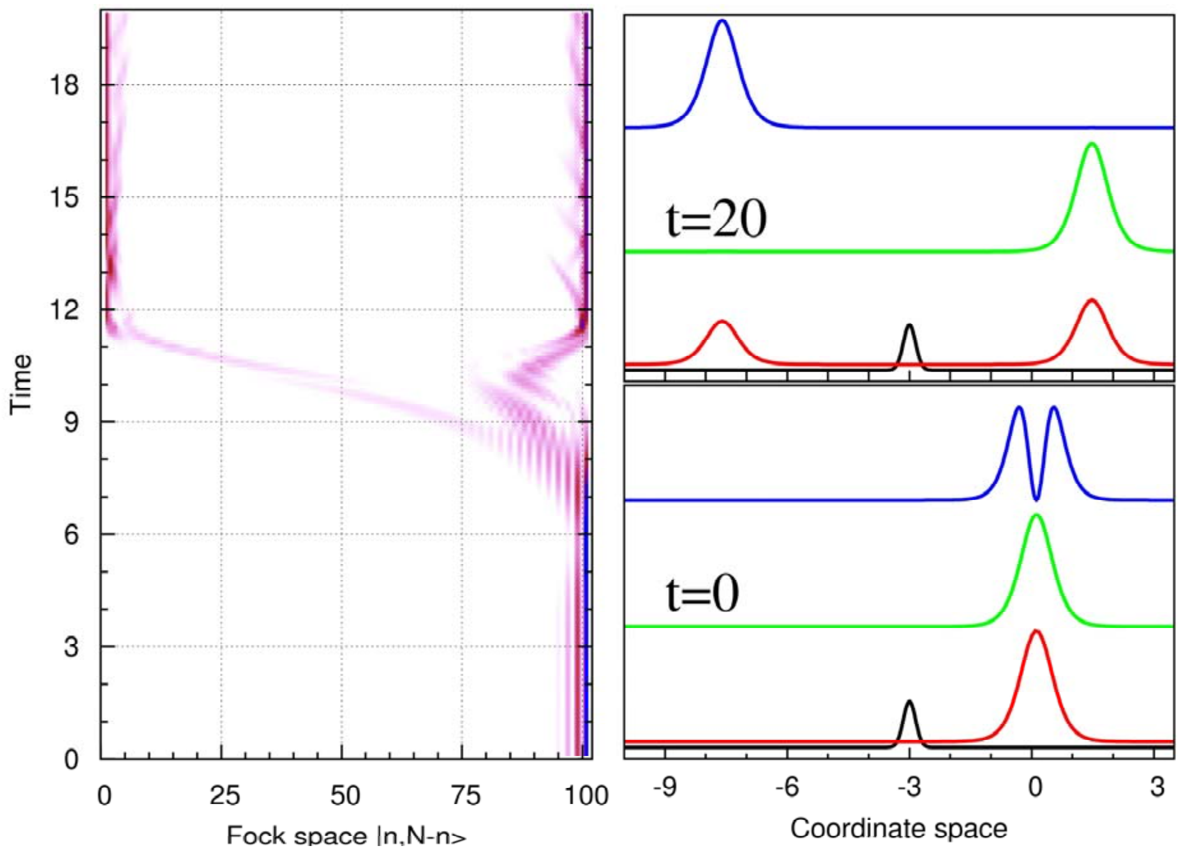

t=20:

mainly |N,0› and |0,N› contribute, respective orbitals are localized at left (blue) and right (green)

t=0:

mainly |0,N› contribute

We call the **Schrödinger cat** state propagating without dispersion and being of fragmented nature **CATon**

Efficient generation of Schrödinger cats, threaded by a potential barrier

CATons II

A.I.S, O.E. Alon, and L.S. Cederbaum,

J. Phys. B: At. Mol. Opt. Phys. 42 091004 (2009)

Initial wave-packet at x=0.1, **barrier** at x=0, V_0=0.3,
Number of orbitals M=4

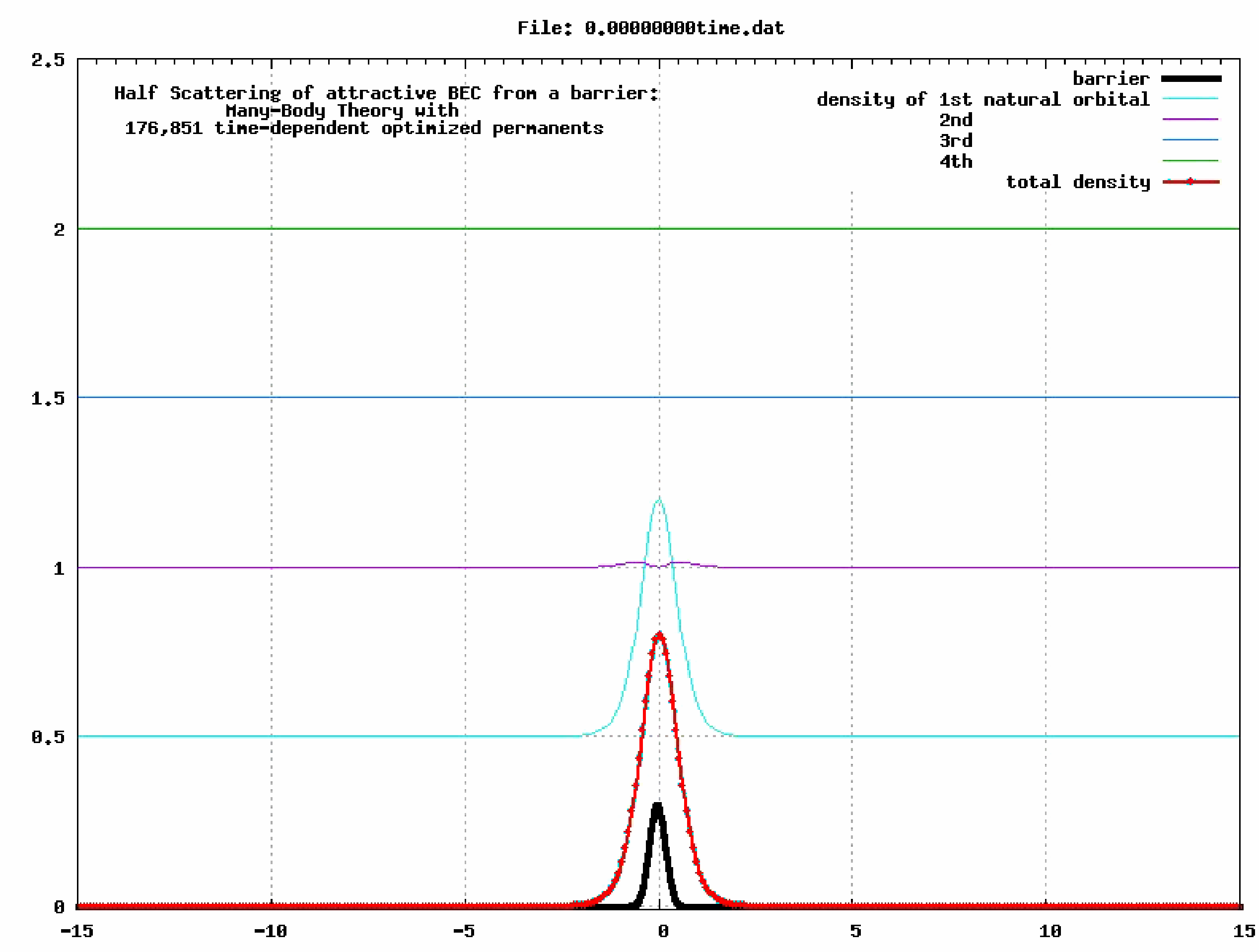

Time-dependent formation of Schrödinger cat state (CATon)

Fate of bright matter-wave soliton trains: from the perspective of many-boson physics

Death of Soliton trains

A.I.S, O.E. Alon, and L.S. Cederbaum,

Time-evolutions of initially-coherent two-hump in-phase solitons: GP (left) vs. Many-Body (right)

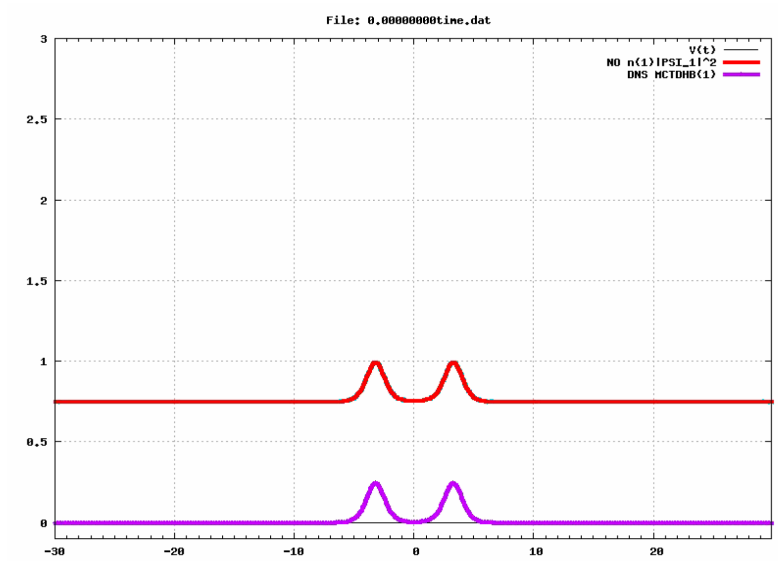

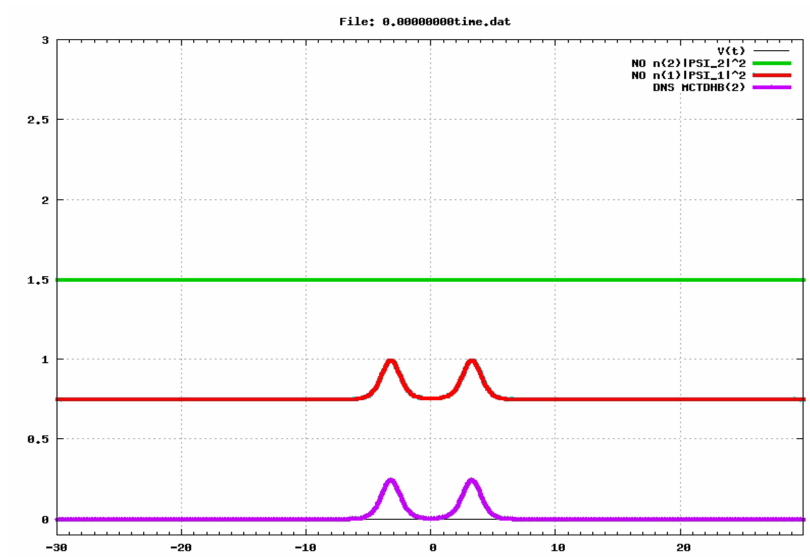

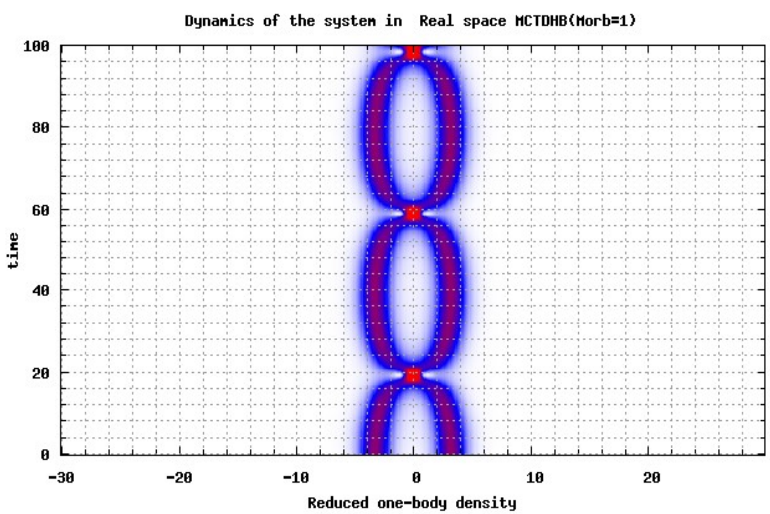

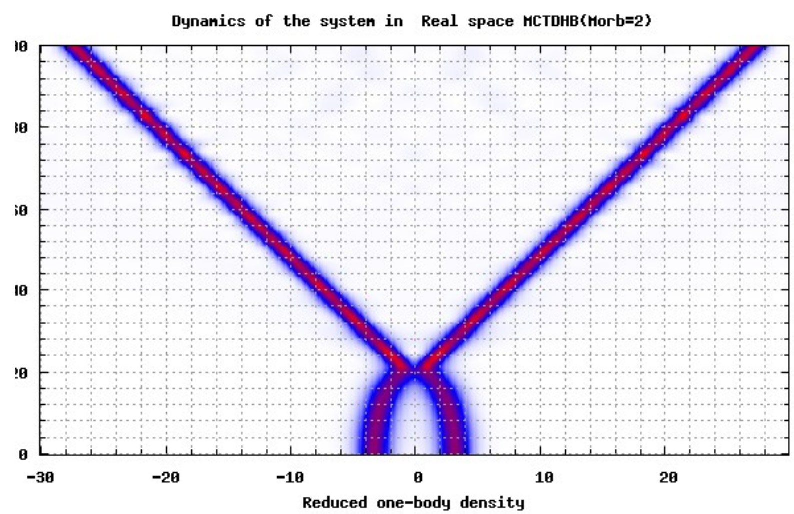

Evolutions of two-hump (a)symmetric in- and out- of phase soliton trains N=2000 in coordinate and momentum spaces: GP(left) and MB(right)

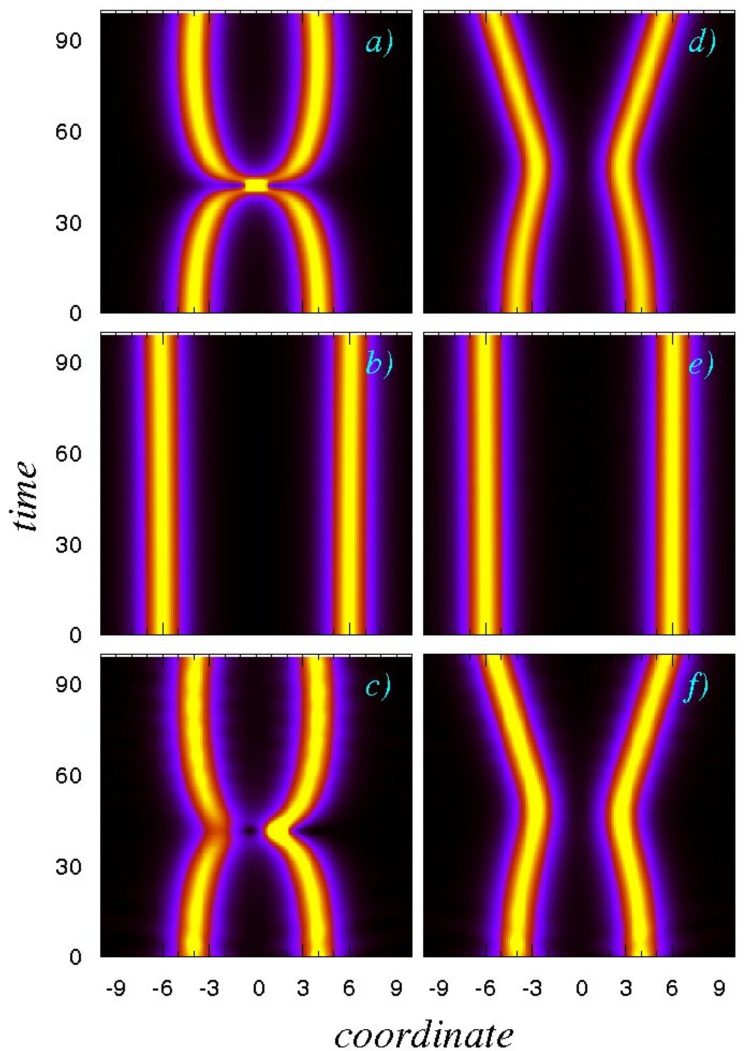

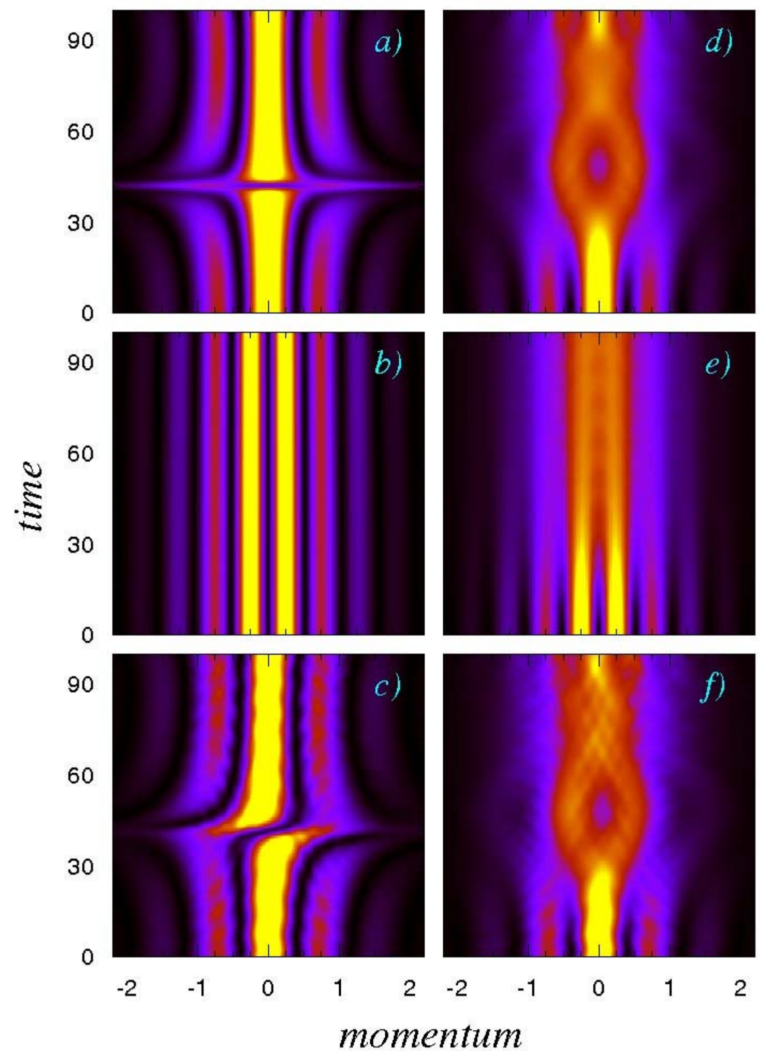

Two-hump symmetric in- and out- of phase soliton trains N=2000 natural occupation numbers and natural orbitals

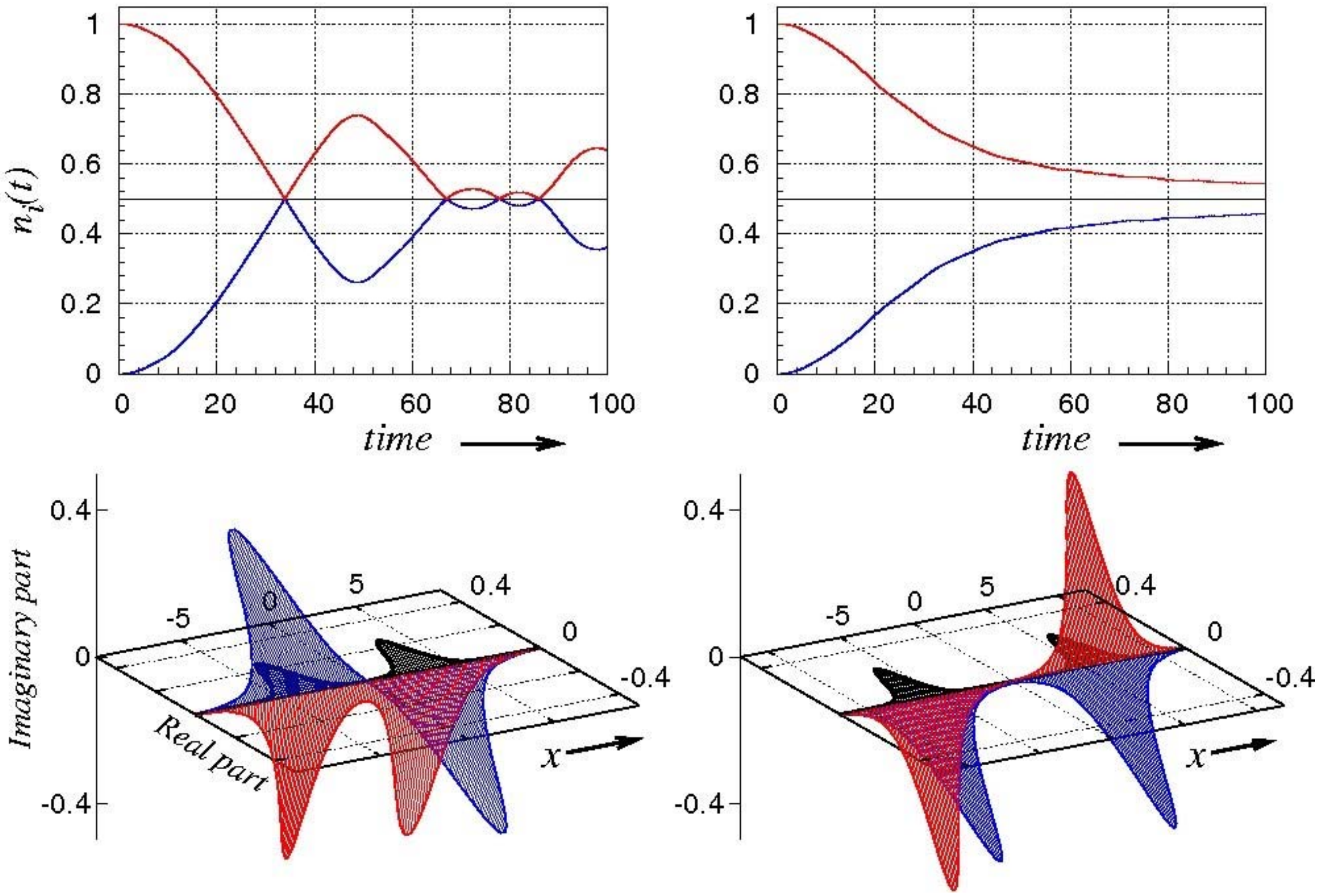

Life Time of two-hump soliton trains

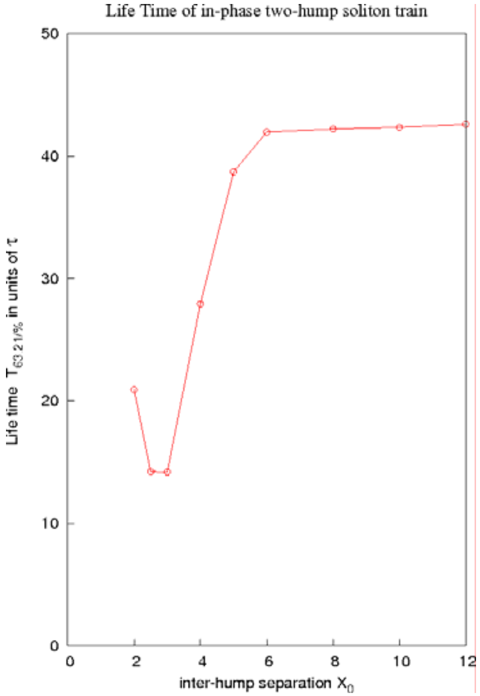

$$g_{1d} = 2\hbar\varpi_r a_s$$

$$\tau = \frac{\hbar^3\Lambda^2}{m\, g_{1d}^2\, N^2}$$

$$\chi = \frac{\hbar^2\Lambda}{m\, g_{1d}\, N}$$

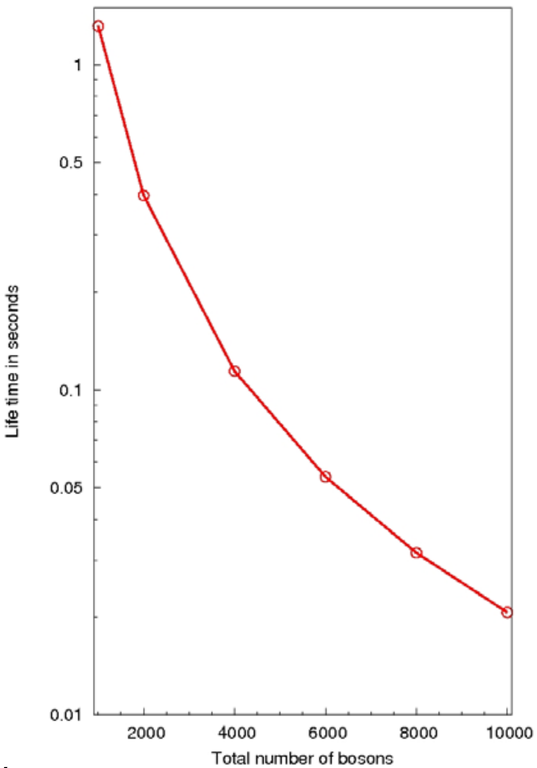

Li^7 : N = 2000;
λ_0= -0.002
ϖ_r = 2π 800 Hz
a_s = -3.0 a_0
τ = 14.21 • 10^{-3} sec
χ = 11.34 • 10^{-6} m

Li^7 : N = 4000
λ_0= -0.001
ϖ_r = 2π 800 Hz
a_s = -3.0 a_0
τ = 3.55 •10^{-3} sec
χ = 5.67 • 10^{-6} m

How to distinguish Solitons and Fragmentons

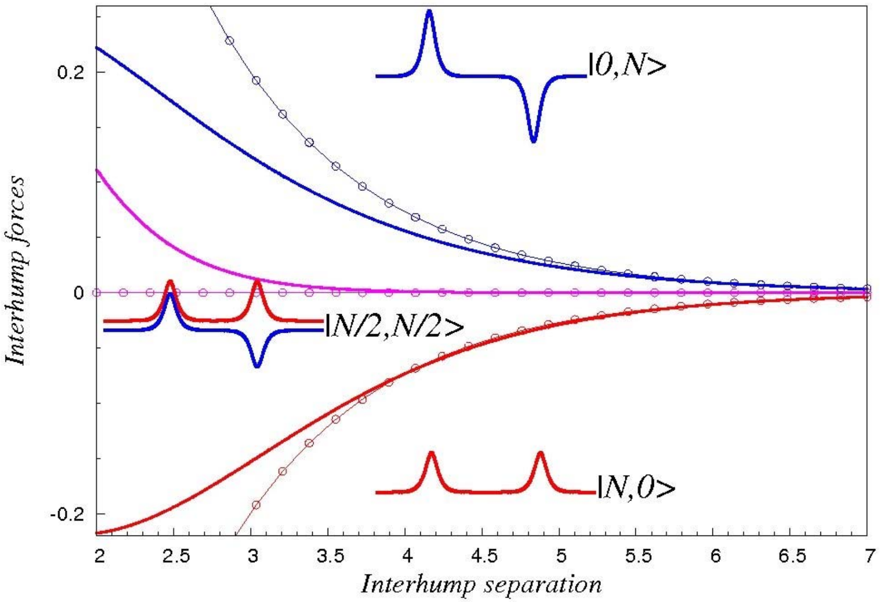

- ✓ Correlation functions for coherent and fragmented states are very different
- ✓ Width of Soliton is broader then that of Fragmenton
- ✓ Inter-hump forces in fragmenton are much weaker

$$F_{Solitons}(\gamma_{GP} = \tfrac{\lambda_0 (N-1)}{4}, X_0) = \pm 4\gamma_{GP}^3 Exp[-2\gamma_{GP} X_0]$$

$$F_{Fragmenton}(\gamma, X_0, n_1, n_2,) = \frac{4(n_1 - n_2)}{3N} 3\gamma^2 Exp[-2\gamma X_0](\lambda_0(\gamma X_0 - 2)(N-1) + 4\gamma^2 X_0 + 5\gamma)$$

Fate of bright matter-wave soliton trains in 1D

- ✓ *The initially coherent multi-hump wave-packets dynamically loose the coherence and become fragmented*
- ✓ *The emerging object is a fragmenton and possesses remarkable properties:*

(1) multi-fold fragmented, i.e., not coherent (condensed)

(2) dynamically stable, i.e., it propagates almost without dispersion

(3) delocalized, i.e., dissociated parts still communicate with one another

Applications (MCTDHB)

Heidelberg:

Ramp-up a barrier: **PRL 99, 030402 (2007);**

Interference: **PRL 98, 110405 (2007)**

Fragmentons: **PRL 100, 130401 (2008);**

Fragmentation in 3D: **PRL 100, 040402 (2008); PRA 82, 033613 (2010)**

CATons: **Formation PRA 80, 043616 (2009) ; Efficient generation JPB, 42 091004 (2009)**

BJJ I: **Exact dynamics of bosonic Josephson junction: PRL 103, 220601 (2009)**

BJJ II: **Attractive vs. repulsive Josephson junctions: PRA 82, 013620 (2010)**

Graz/Vienna:

Optimal control of number squeezing: **PRA 79, 021603 (2009), PRA 80, 053625 (2009);**

Interferometry: **NJP 12, 065036 (2010) ;**

Just started: Hamburg, Vienna II,...,

want to join?

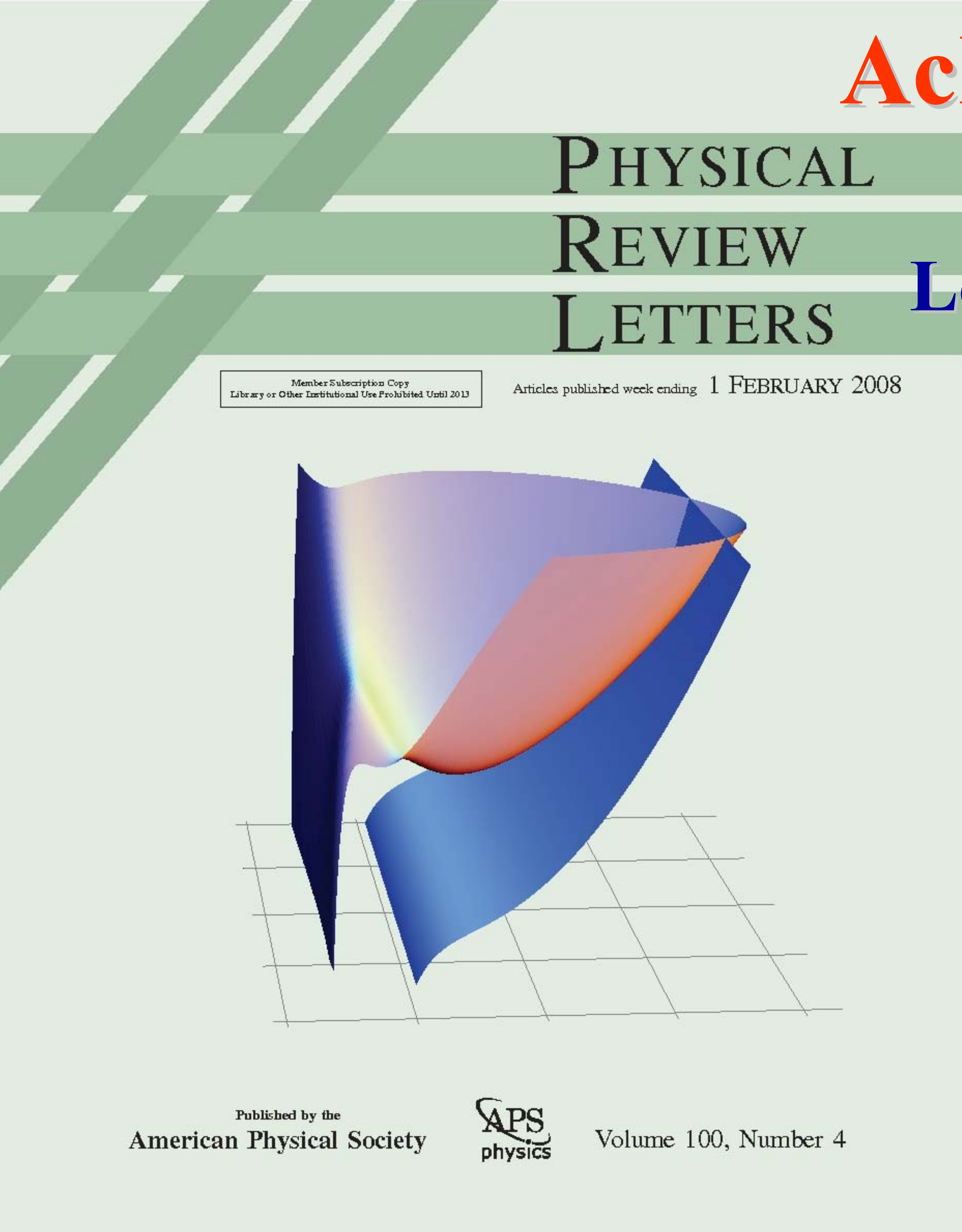

Acknowledgments

Lorenz S. Cederbaum
Ofir E. Alon

Kaspar Sakmann

Hans-Dieter Meyer

Marios C. Tsatsos
Axel U. J. Lode